PROCEEDINGS OF SCIENCE

A magnified view of galaxy formation

Tucker Jones[*†]
Institute for Astronomy, University of Hawaii
E-mail: tucker.jones@hawaii.edu

Distant galaxies are difficult to study because of their small angular size and faint apparent brightness. I discuss observations of gravitationally lensed galaxies which are highly magnified, providing superior sensitivity and spatial resolution. These data reveal a wealth of information about galaxy physical properties and evolution during their most active period of formation at redshifts $z = 1$–3. Spatially resolved spectroscopic data indicate that most galaxies at this epoch are forming stars in gravitationally unstable, turbulent disks. Gas-phase metallicity is a particularly valuable diagnostic of gas content and inflow/outflow which regulate the growth of galaxies, with observations indicating relatively high gas fractions and outflow rates. Looking forward, dedicated surveys of lensed galaxies from large telescopes on the ground and in space are dramatically increasing our knowledge of galaxy physical properties at early times and the processes by which they evolve.

Frank N. Bash Symposium 2015
18-20 October
The University of Texas at Austin, USA

[*]Speaker.
[†]Hubble Fellow

PoS(BASH2015)013

1. Introduction

Large imaging surveys with the Hubble Space Telescope (such as the HUDF [1], GOODS [2], COSMOS [3], and CANDELS [4]) and other facilities have revealed diverse and evolving galaxy populations as a function of cosmic time, extending to within a billion years of the Big Bang at redshifts $z > 8$. The redshift range $z = 1$–3 (lookback times of $\sim$10 billion years) has been of particular interest over the past decade as it corresponds to the peak epoch of star formation activity [5] and hence galaxy growth. It is also during this period that regular kinematic and morphological structure emerges in the form of symmetric disk and spheroidal components [6, 7], in contrast to predominantly chaotic morphologies at $z > 2$. Meanwhile, theoretical work and numerical simulations have helped to connect the galaxy population to progenitors and descendants at different times through through techniques such as halo abundance matching [8]. This provides a statistical description of evolution in stellar mass, star formation rate, size, and morphology, particularly for the most massive and luminous galaxies.

With a census of the galaxy population and its overall evolution in place, attention has turned to understanding the physical mechanisms by which galaxies evolve. This includes the role of mergers, star formation, dynamical evolution, and gaseous outflows driven by feedback from star formation and accreting black holes. Characterizing these processes requires spatially resolved measurements of individual galaxies. This presents the principal challenge in understanding galaxy evolution at early times: Hubble's diffraction limit corresponds to $\sim$1 kpc at $z = 1$–3, comparable to the size of typical galaxies at this epoch. Good spatial sampling is obtained only for the most massive galaxies with $M_\star \gtrsim 10^{10} M_\odot$ whose effective radii are typically $\sim$2 kpc [9]. Ground-based integral field spectrographs can map emission line flux and kinematics with the same angular resolution as Hubble by using adaptive optics (AO) to correct for atmospheric seeing. AO-assisted data sets illustrate the necessity for $\sim$kpc resolution to accurately characterize kinematics of massive galaxies at these epochs [10], while the bulk of the population at $M_\star \lesssim 10^{10} M_\odot$ are difficult to detect and are poorly resolved.

Strong gravitational lensing offers a means to achieve higher signal-to-noise and improved spatial sampling by observing highly magnified sources. In practice, magnification factors can often exceed $\mu \gtrsim 10$ [11] corresponding to a 10-fold increase in the number of spatial elements, or a 10-fold increase in signal/noise for unresolved data. This provides physical resolution as high as $\sim$100 pc for observations with Hubble or ground-based AO – a tremendous advantage over blank-field surveys. Figure 1 illustrates a spectacular example whereby the kinematics and morphology of an intrinsically compact galaxy are accurately characterized thanks to strong lensing magnification. In the following sections I describe how lensed galaxies are discovered and characterized (§2), advances in the field of galaxy evolution from lensing studies (§3), and the exciting potential of ongoing and future work with gravitational lensing (§4).

2. Strong lensing surveys

Gravitational lensing occurs when a massive object is located near the line of sight between the observer and a background source, causing light from the background source to be deflected. This proceeding is concerned with the case of strong lensing in which multiple images are formed,

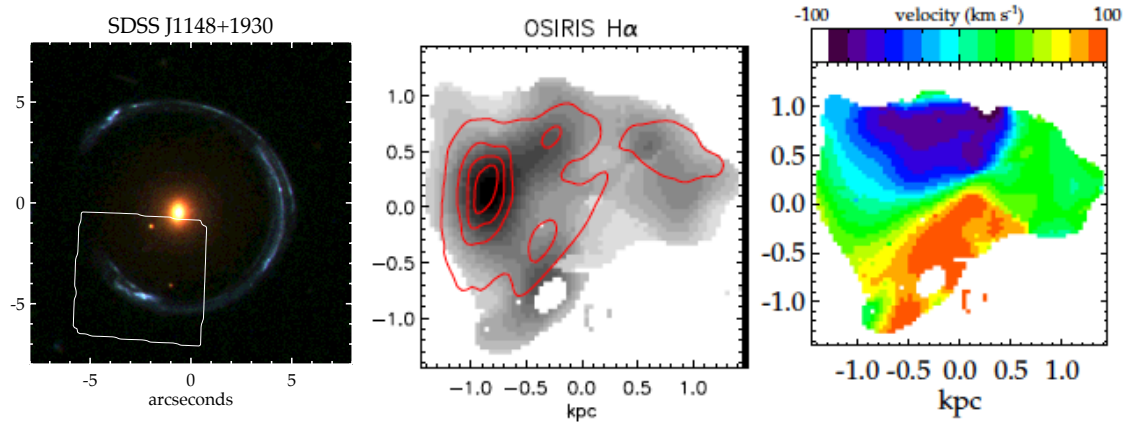

Figure 1: An example of the benefits of studying gravitationally lensed galaxies, from Jones et al. [40]. The left panel shows a Hubble image of a blue background galaxy at $z = 2.38$ magnified by a factor of $\sim$30 by a massive red foreground elliptical at $z = 0.44$, resulting in nearly complete Einstein ring. The lensed galaxy was observed with the Keck/OSIRIS integral field spectrograph (in the region shown by the white box) to map the star formation, kinematics, and gas-phase metallicity. Reconstructed in the source plane, the data reveal a complex and well-sampled distribution of star formation (center panel; grey: Hα, red contours: ultraviolet continuum) and a regular rotating velocity field (right panel). This structure would not be discerned at the $\sim$1 kpc resolution achieved for non-lensed sources.

with magnification factors $\mu > 2$. For a point mass M located directly along the line of sight, the background source will be lensed into a ring with angular radius

$$\theta_E = \sqrt{\frac{4GM}{c^2}\frac{D_{LS}}{D_L D_S}} \tag{2.1}$$

where D_L, D_S, D_{LS} are the observer-lens, observer-background source, and lens-background source angular diameter distances, respectively. Massive galaxies at intermediate redshifts can act as lenses with $\theta_E \gtrsim 1$ arcsecond [12] while galaxy clusters can exceed $\theta_E > 30$ arcseconds [13]. The example in Figure 1 is an intermediate group-scale halo lens with $\theta_E \approx 5$ arcseconds.

The utility of galaxies and clusters as strong lenses was first pointed out by Zwicky in 1937 [14] and is clear from Figure 1. However, strong lensing systems have only been discovered and exploited since 1979 [15]. Strong lensing has since been used for many scientific purposes including constraints on cosmological parameters via time delays [16] and frequency statistics [17], the mass profiles of dark matter halos associated with galaxies and clusters [18, 19], and high resolution studies of lensed galaxies as discussed in this proceeding. All of these applications depend critically on being able to identify samples of lensing systems and accurately model the lensing mass distribution. Several techniques have been developed to model lensing systems and to reconstruct lensed galaxies in their source planes; interested readers are referred to the review by Lefor et al. [20] as well as individual papers discussed here. Below I briefly review some of the techniques used to find lensed galaxies.

2.1 Cluster lenses

Massive galaxy clusters at intermediate redshifts are excellent strong lensing systems. By

virtue of their large lensing deflection angles compared to the background source density, essentially all such clusters act to strongly lens multiple background sources. Large samples of lensed galaxies can therefore be obtained from simple deep imaging surveys of distant rich clusters. For example, a search of archival Hubble imaging of galaxy clusters in 2005 yielded a sample of over 100 highly magnified galaxies lensed into elongated arcs [21]. Cluster surveys based on X-ray (e.g., MACS and its successors [22]) and red-sequence (e.g., RCS and RCS-2 [23]) identification have been particularly effective. Most recently, the Hubble Frontier Fields initiative[1] is acquiring ultra-deep imaging of six of the most efficient known strong lensing clusters (with the largest known θ_E), resulting in $\gtrsim 50$ individual lensed galaxies identified behind each cluster [24].

2.2 Galaxy-scale and group-scale lenses

Galaxies which act as strong gravitational lenses are much harder to find than clusters, since their lensing cross sections are small compared to the background source density. Nonetheless large samples of galaxy-and group-scale lenses have been identified by a variety of methods. The simplest approach is to search large-area imaging surveys for objects which visually appear to be strongly lensed. Efforts in Hubble imaging fields [25] and the Sloan Digital Sky Survey [26, 27, 28] have uncovered well over 100 such galaxies, which tend to be much brighter (in both intrinsic and apparent luminosity) compared to cluster lensing samples. Additionally, such imaging surveys are prone to false positives particularly in seeing-limited surveys, and hence improved imaging or spectroscopy is needed for confirmation [29]. The SLACS survey [12] used a slightly different approach to identify lens systems in Sloan by following up objects with multiple spectroscopic redshifts, yielding a high detection rate of small-separation ($\theta_E \lesssim 1.5$ arcsecond) galaxy lenses. Yet another successful method is to identify extremely bright objects which are more numerous than expected from the intrinsic luminosity function of a population. This is particularly effective at far-IR through millimeter wavelengths [30, 31, 32].

3. Structure and evolution of lensed galaxies

I now turn to a review of what has been learned about galaxy evolution by studying strong lensing systems. The present section focuses on structure and evolution of galaxies at $z \simeq 1$–3 for the practical reason that this redshift range is amenable to a variety of key observational probes, and is also of interest as the peak epoch of galaxy and supermassive black hole growth. For the largest galaxies, Hubble imaging provides good spatial sampling of the stellar population (mass, star formation rate, star formation history) via rest-frame ultraviolet and optical photometry. Ground-based spectrographs with adaptive optics (and to some extent Hubble's near-infrared grisms) can map emission lines at similar resolution to determine the kinematics, metallicity, and distribution of star formation. Millimeter-wave interferometers have recently become sensitive enough to detect molecular gas and dust continuum in the most active systems. Progress in all of these areas is accelerating thanks to the increasing discovery rate and diversity of lensed galaxies via the methods described in §2.

[1] http://www.stsci.edu/hst/campaigns/frontier-fields/

3.1 Kinematics and morphology

Galaxy morphologies at high redshifts $z \gtrsim 2$ are typically irregular with no clear disk or spheroidal components [6]. As such it is not immediately clear whether they are supported by rotation (leading to a disk morphology), random motions (spheroid), or perhaps lack dynamical equilibrium due to high accretion and merger rates. The advent of near-infrared integral field unit (IFU) spectrographs coupled with adaptive optics systems now enables direct kinematic measurements at high redshifts by mapping strong nebular emission lines, in particular Hα and [O III]λ5007. Initial observations reported in 2006 revealed velocity gradients [33] but lacked adaptive optics. With 4 kpc resolution, these data could not clearly distinguish between mergers and rotating disks. Later that year, the first observations of a lensed galaxy at $z = 3.2$ showed clear rotation with ∼200 parsec spatial resolution [34], sufficient to characterize the rising inner rotation curve. Early AO-assisted observations achieved ∼1 kpc resolution and likewise found rotational kinematics in more massive non-lensed galaxies [35, 36]. These early results are exemplary of the role that lensed galaxies have continued to play in understanding the internal structure of galaxies at high redshift.

A consensus picture of galaxy kinematics at $z \simeq 2$ has gradually emerged over the past decade: the majority of star forming galaxies are characterized by turbulent, gravitationally unstable thick disks while approximately 30% are undergoing mergers. This has been clear for some time for the larger and more massive population which is reasonably well sampled with AO or in very good seeing [37]. Lower-mass galaxies tend to be spatially more compact and showed little evidence of ordered velocity gradients in early data sets [37, 38]. However, modest samples of lensed galaxies revealed systemic rotation in these sources which would not be detected at the lower sensitivity and coarser resolution of non-lensed data sets [11, 39]; Figures 1 and 2 are two such examples. Deeper AO-assisted followup observations later confirmed rotational motion to be ubiquitous even among compact sources [10].

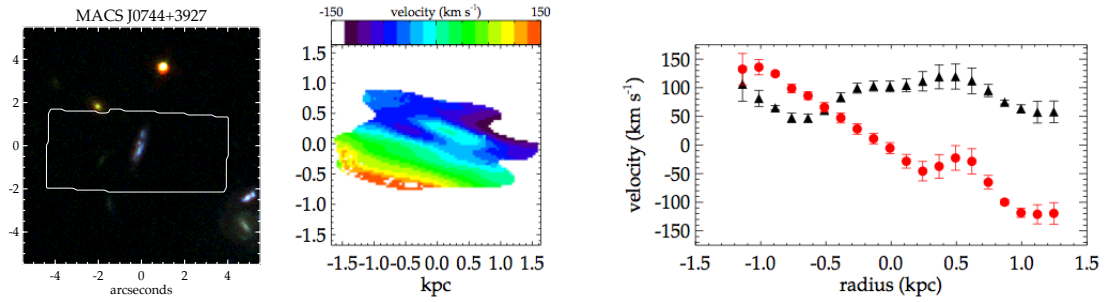

Figure 2: Kinematics of a compact gravitationally lensed galaxy, from Jones et al. [40]. The left panel shows a Hubble image of a $z = 2.21$ galaxy (image center) lensed by the cluster MACS J0744. As with Figure 1 this galaxy was observed with the Keck/OSIRIS integral field spectrograph and adaptive optics in the region shown by the white box. The source is well-sampled, subtending ∼10 spatial resolution elements with both OSIRIS and Hubble. Reconstructed in the source plane (center panel), the galaxy is intrinsically compact with a radius of only ∼1.5 kpc. A strong velocity gradient is seen in the Hα emission line centroids shown with the color scale, indicating large-scale rotation. The right panel shows one-dimensional rotation (red circles) and velocity dispersion (black triangles) curves extracted along the kinematic major axis. Local velocity dispersions are 50–100 km s^{-1}, comparable to the rotation velocity.

While the majority of star formation in $z \simeq 2$ galaxies occurs in a rotating disk, their properties are substantially different from spiral galaxy disks at $z = 0$. Perhaps most notably their local velocity dispersions are typically $\sigma \approx 50$–100 km s^{-1} even in the outer regions (e.g., Figure 2), far higher than in nearby spirals ($\sim$10 km s^{-1}). This indicates large disk scale heights of $\sim$1 kpc, in broad agreement with relatively small axis ratios inferred from high-resolution Hubble imaging [41]. Velocity dispersions show little variation among the entire observed population at high redshift. In contrast, circular rotation velocities vary significantly. Rotation velocities are on average higher for galaxies of larger size (Figure 3) and stellar mass [42]. Nonetheless random motions are significant with $V_{\rm rot}/\sigma < 10$ even in the largest galaxies at $z \simeq 2$, while random motions are dominant in many of the compact and lower-mass galaxies with $V_{\rm rot}/\sigma < 1$.

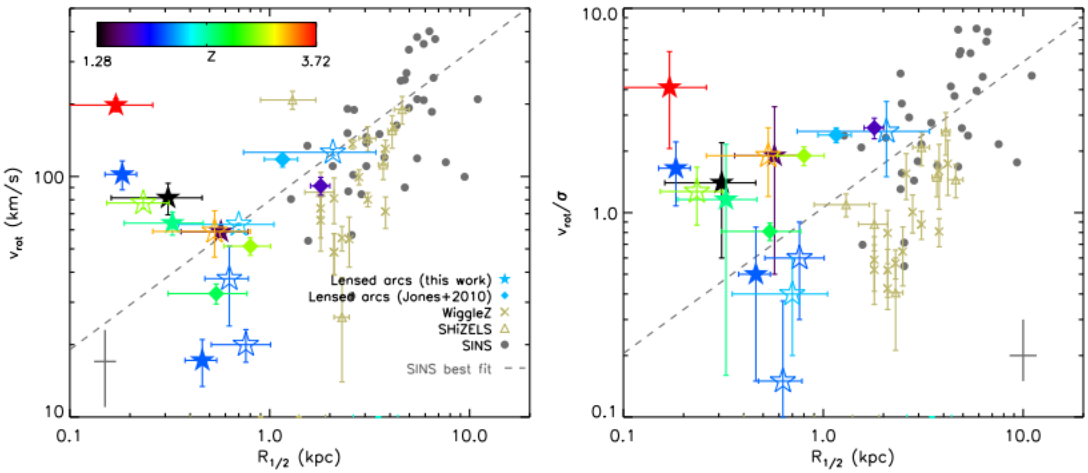

Figure 3: High redshift galaxy kinematic properties, reproduced from Livermore et al. [42]. *Left:* circular rotation velocity as a function of half-light radius. *Right:* ratio of rotational to random motion, $V_{\rm rot}/\sigma$, as a function of half-light radius. Lensed galaxies are color-coded according to their redshift with filled symbols indicating those with ordered rotation, and open symbols for galaxies undergoing mergers or not showing signs of rotation. In the latter cases $V_{\rm rot}$ corresponds to half of the total velocity shear. A key point of this figure is that non-lensed surveys (e.g., WiggleZ, SHiZELS, SINS) are unable to probe galaxies smaller than $R_{1/2} \lesssim 1.5$ kpc, corresponding to the diffraction limit. Lensed galaxies successfully extend this limit to characterize the more common population of intrinsically smaller sources. Dashed lines show a fit to the SINS adaptive optics sample from Newman et al. [10]. Lensed galaxies lie along an extrapolation of this trend albeit with large scatter.

Another key difference between local and high redshift galaxies is the distribution of star formation. Star-forming H II regions at high redshift are almost never organized in spiral arms, and the few cases which do show spiral structure still have high $\sigma \gtrsim 50$ km s^{-1} [43, 44]. Instead, nearly all star forming galaxies at high redshift contain multiple giant H II regions (often called "clumps") which dominate the morphology of both nebular emission lines and far-ultraviolet continuum. Figure 1 shows a representative example of clumpy structure. In the most massive galaxies, these clumps can reach $\sim$1 kpc in size such that they are marginally resolved [45, 36, 46]. Targeted studies of lensed galaxies, including Hα narrowband imaging with Hubble, have resolved clumps spanning over a decade in size and nearly three decades in luminosity [11, 47, 42] as shown in

Figure 4. While giant H II regions of similar size can be found in nearby galaxies, they are more frequent and typically have far higher star formation rate densities at higher redshifts.

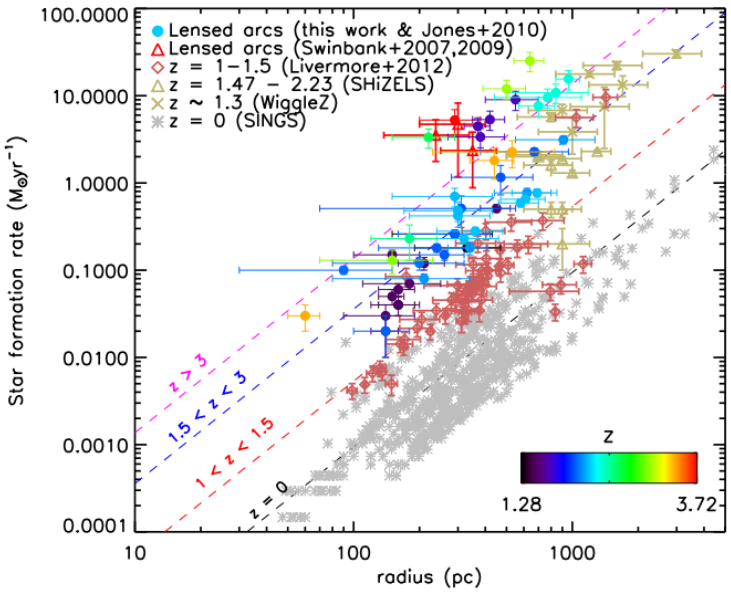

Figure 4: Size and star formation rate of giant H II regions as a function of redshift, reproduced from Livermore et al. [42]. Lensed objects are color-coded according to their redshift. High densities of star formation in giant H II regions at $z = 1$–5 suggest higher gas density and/or star formation efficiency compared to nearby galaxies.

The distinguishing features of rotating galaxies at high redshifts – namely high velocity dispersion and prevalent giant H II regions – are explained by violent gravitational instabilities. The stability of a rotating system can be described by the Toomre parameter

$$Q = \frac{\sigma\kappa}{\pi G\Sigma} \tag{3.1}$$

where σ is the radial velocity dispersion, κ is the epicyclic frequency, Σ is the mass surface density, and G is the gravitational constant. Values less than a critical $Q_{crit} \approx 1$ indicate an instability where the combined orbital motion and dispersion are insufficient to support the total mass. This leads to collapse on spatial scales

$$L_J = \frac{\pi\sigma^2}{8G\Sigma}. \tag{3.2}$$

Galaxies across a wide range of stellar mass, size, and $V_{\rm rot}/\sigma$ consistently have values of Q near or below unity indicating that they are likely unstable to localized gravitational collapse [36, 11, 40]. The Jeans scale for collapse, L_J, is consistent with the sizes of the largest star-forming clumps although the uncertainties are of order a factor of two. These clumps are known to be short-lived based on the smoothness of stellar mass compared to star formation distributions, indicating lifetimes ∼100–200 Myr [9] corresponding to a few dynamical timescales. There are two plausible explanations for clump destruction. If clumps remain gravitationally bound, their overdensity relative to the surrounding disk will cause the clumps to migrate inward via dynamical friction [48],

contributing to growth of a stellar bulge. This is an appealing way to explain the buildup of bulges in massive galaxies by $z \simeq 1$. However, feedback from the intense star formation within clumps drives large-scale outflows of gas with mass. Such outflows have been localized to individual clumps in some cases [49, 50], with high mass loading factors $\eta = \dot{M}_{outflow}/\mathrm{SFR}$ possibly exceeding unity. Such rapid mass loss may cause the clumps to disrupt before they can migrate into bulge-like orbits.

Theoretical work provides further support for widespread unstable disks within high redshift galaxies. Cosmological simulations with hydrodynamics suggest that the majority of mass is accreted in a relatively smooth manner [51, 48, 52], with mergers of mass ratio greater than 1:10 accounting for only $\sim$1/3 of accreted mass. The smoothly accreted component carries angular momentum and naturally settles into a disk, while the high specific accretion rates at $z \simeq 2$ lead to giant clumps formed through disk instability [53, 54]. As with observational results, it is not clear from the simulations whether clumps are disrupted on short timescales due to feedback [55] or migrate inward to form a bulge [56, 57]. A better understanding of stellar feedback is needed to resolve this issue and determine the origin of bulge growth at high redshifts. Meanwhile the gravitationally unstable thick disk scenario provides a successful framework for understanding the observed properties of most galaxies at $z \simeq 2$.

3.2 Gas content

The high specific star formation rates of galaxies at high redshifts suggest high gas fractions relative to galaxies in the nearby Universe. High gas fractions are likewise required to explain the luminosity function of giant star-forming clumps [47]. A crude estimate of the gas content can be made by inverting the Kennicutt-Schmidt law, indicating baryonic gas fractions of $\sim$50% (i.e., $\mathrm{M_{gas}} \approx \mathrm{M_*}$ [58, 40]). This is broadly consistent with the difference between stellar and dynamical masses. Early direct measurements of molecular gas inferred similar results but highlighted the difficulty inherent in converting from a rotational CO line luminosity to a total molecular gas mass [59, 60]. While large observing campaigns have obtained CO emission measurements for dozens of $z > 1$ galaxies [61], few are spatially resolved and hence there is only limited information on the gas distribution and kinematics. This is true even for the several tens of lensed galaxies which have now been detected in molecular CO transitions [62, 31, 63]. Nonetheless lensed galaxies have successfully probed a large dynamic range of galaxy properties, revealing scaling relations of molecular gas with galaxy stellar mass and redshift [63].

The Atacama Large Millimeter Array (ALMA) is expected to make tremendous progress in mapping the distribution and kinematics of molecular gas in distant galaxies. Although still in its early science phase, ALMA has already demonstrated an order of magnitude improvement in both sensitivity and angular resolution compared to previous millimeter-wave instruments. The most detailed information available on molecular gas in galaxies at high redshift comes from spatially resolved observations of a mere handful of gravitationally lensed galaxies observed with ALMA. Perhaps most impressive among these are data obtained for a strongly lensed galaxy at $z = 3.0$ during long baseline commissioning [64]. The combination of lensing magnification and baselines of up to 15 km provided $\sim$20–50 pc resolution imaging of the far-infrared continuum and CO line emission at millimeter wavelengths. Several clumps of molecular gas and dust emission are seen, with properties similar to UV- and optically-selected clumps of star formation described in

the previous section (e.g. Figure 4). Similar clumps have been observed in other lensed sources at $z = 2.0$ and $z = 2.3$ in multiple emission lines from CO and fine-structure metal transitions, from which ambient physical conditions of the interstellar medium are derived [65, 66]. Kinematics in all cases are consistent with a turbulent thick disk, and in one case the molecular gas morphology can be directly compared to that of the star formation traced by Hα and UV continuum (Figure 5). The gas and star formation distributions are similar, consistent with clumpy star formation arising from gravitational instability in a gas-rich disk. The available molecular gas data therefore support the picture described in the previous section whereby most $z \simeq 2$ galaxies are characterized by turbulent gas-rich disks, with gravitational instability leading to giant clumps of gas and star formation. ALMA is now fully capable of verifying this picture with larger samples, particularly of lensed galaxies.

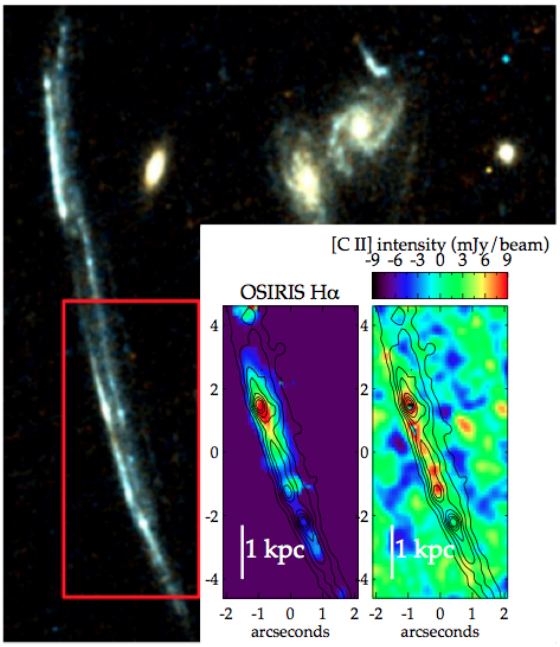

Figure 5: A lensed $z = 2.01$ galaxy observed with spatially resolved measurements of the molecular and ionized gas phases. The background Hubble color composite image shows the elongated arc which extends over 20 arcseconds. The red box corresponds to the two insets which show maps of Hα emission obtained with Keck/OSIRIS and adaptive optics (reported by Jones et al. [11]) and [C II]λ158 μm emission obtained with ALMA (reported by Schaerer et al. [66]). The photodissociated molecular gas traced by [C II] appears to be co-spatial with the giant H II regions traced by Hα and UV continuum emission (shown as contours in the inset panels).

3.3 Metallicity and gas flows

Gas flows are an important aspect of galaxy evolution, as has been noted in the previous sections. Galaxy growth from cosmological accretion and mergers is balanced by feedback from various forms of energy associated with star formation and accretion onto supermassive black holes. This feedback drives strong outflows of gas and dust which are observed in essentially all star forming galaxies at $z \gtrsim 2$ [67, 68, 69]. The rates of gas inflow and outflow are extremely difficult

to measure observationally, although outflow rates comparable to or even in excess of the ongoing SFR are inferred from a few lensed galaxies with exceptional quality spectra [70]. Cosmological simulations show that strong feedback is required to match the stellar mass function of galaxies, but do not strongly constrain the feedback mechanism or gas flow rates [71]. Gas-phase metallicity offers a promising observational probe as it is sensitive to the history of gas inflow, outflow, and star formation rate [72, 40]. Figure 6 shows the results of a simple analytic model describing how inflow and outflow affect gas-phase metallicity, along with data from both lensed and non-lensed galaxies at $z \simeq 2$. The data can only be explained with sufficiently high gas fractions, mass outflow rates, or both. The inferred gas fractions and/or outflow rates decrease for galaxies of higher stellar mass, possibly indicating that feedback is more efficient at ejecting gas and metals from lower-mass galaxies due to their weaker gravitational potentials. Another possibility is that feedback changes from a primarily momentum-driven mode at high mass to energy-driven at low mass [73]. Notably, the galaxy masses reached with lensing in Figure 6 are well below that achieved by non-lensing surveys, which rely on stacking to probe this transitionary mass range. Individual lensed galaxies are needed to probe the scatter at low mass which may increase depending on the mode of feedback [74]; this has yet to be tested with rigorous observations.

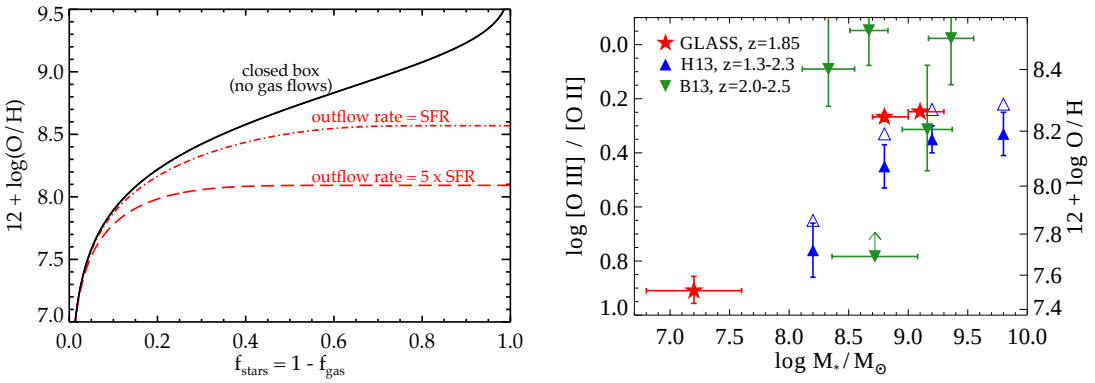

Figure 6: *Left:* Results from a simple chemical evolution model described by Jones et al. [40]. Metallicity (i.e. gas-phase oxygen abundance) is shown as a function of stellar mass fraction (or equivalently gas fraction) for outflow mass loss rates of 0, 1, and 5 times the star formation rate. Solar metallicity is $12 + \log(\mathrm{O/H}) = 8.69$ in these units. As gas is converted into stars, metallicity increases at a rate modulated by the degree of mass loss. *Right:* Metallicity as a function of stellar mass for galaxies at $z \simeq 2$, from Jones et al. [75]. Metallicities are derived from nebular emission lines, in this case using [O III] and [O II]. Blue triangles are from composites of non-lensed galaxies demonstrating a steep mass-metallicity relation especially at masses below 10^9 $\mathrm{M}_\odot$. Green and red data points represent individual gravitationally lensed galaxies which follow the overall trend with non-zero scatter. The low metallicities – reaching $10\times$ below solar in some cases – indicate high gas fractions $f_{\mathrm{gas}} > 0.8$ and/or outflow rates of several times the SFR according to the model shown at left.

Radial gradients in the gas-phase metallicity provide further constraints on feedback and gas flows. Local galaxies are observed to have modest gradients with higher metallicity in the central regions [76]. Numerical simulations show that multiple forms of feedback act to flatten radial metallicity gradients in star-forming disks [77, 78]. Simulations with different feedback prescriptions can match observations at $z = 0$ and predict different behavior at higher redshift, such that

observations at $z > 1$ provide a direct test. To date several measurements have been made for gravitationally lensed galaxies which provide the most reliable results due to their high spatial resolution [75, 79, 80]. A growing number of non-lensed galaxies also have limited spatially resolved metallicity measurements which show interesting trends with global demographic properties [81]. Figure 7 shows a summary of current observational results compared to theoretical predictions, with a diversity of gradient slopes and a corresponding range of plausible feedback scenarios.

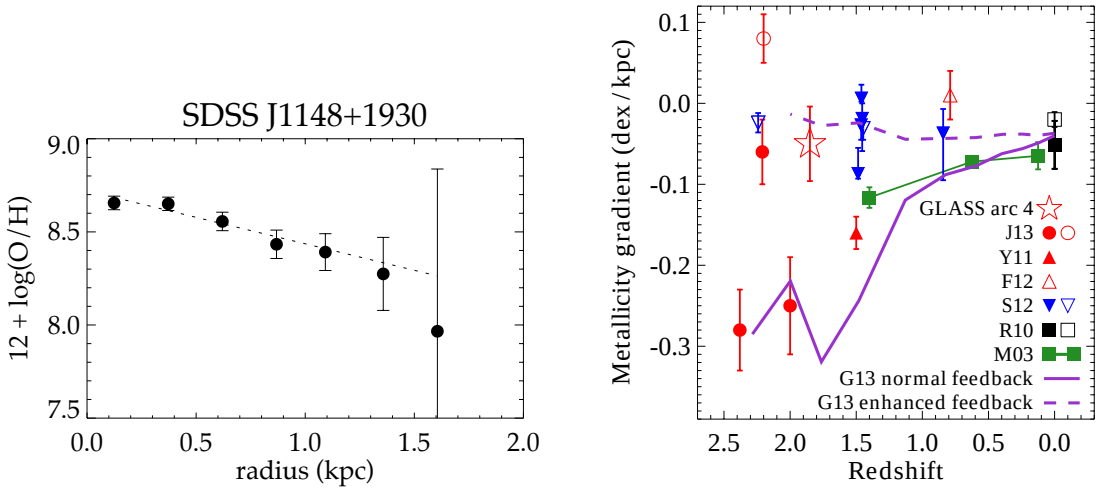

Figure 7: *Left:* Gas-phase metallicity as a function of galactocentric radius for the lensed $z = 2.4$ galaxy shown in Figure 1, from Jones et al [40]. A negative gradient is apparent with a slope of -0.28 dex/kpc. *Right:* Metallicity gradients in star forming galaxies as a function of redshift, from Jones et al. [75] (see also Leethochawalit et al. [79]). Red points are gravitationally lensed galaxies while blue points are non-lensed galaxies observed with adaptive optics such that the effective disk radii are resolved. Purple lines show results from simulations with a "standard" feedback prescription (solid) and a stronger "enhanced" feedback resulting in higher rates of mass and metal loss (dashed). The more rapid mass loss and subsequent re-accretion leads to more efficient gas and metal mixing and hence flatter gradients (closer to zero slope) in the more enhanced feedback case. Existing data show a range of results which are approximately bracketed by the two feedback models shown here.

4. Conclusions and future outlook

Strong gravitational lensing has played an important role in developing the current paradigm of galaxy evolution by probing intrinsically fainter sources and smaller spatial scales than is otherwise possible at cosmological distances. Within a decade, the next generation of thirty-meter class optical/infrared telescopes are expected to provide similar gains in resolution and sensitivity for the entire galaxy population. More exciting is the prospect of obtaining resolution approaching 10 parsecs for strongly lensed galaxies with these facilities and with ALMA [64]. Such data will address a new set of questions by directly measuring properties such as the central density profiles of dwarf galaxies, supermassive black hole masses, outflow launching sites, escaping ionizing radiation, and other quantities at high redshifts.

Several parallel efforts are underway to discover and characterize larger samples of lensed galaxies. The Hubble Frontier Fields (HFF) initiative is a recent example with remarkable success in its goal of using cluster lenses to detect the faint sources responsible for cosmic reionization at $z > 7$ [82, 83, 84]. HFF draws on previous and contemporary cluster surveys including MACS [22], CLASH [85], SURFSUP [86], and GLASS [87], with particular care given to constructing accurate gravitational lens models [88]. Meanwhile the EMACS program is uncovering even more powerful cluster lenses for future surveys [89]. For galaxy- and group-scale lenses, visual classification projects such as the citizen science survey Space Warps [90] are expected to discover large samples in current SDSS data, future LSST data, and other surveys. These growing samples of gravitational lenses, combined with powerful existing and near-future facilities, will define the cutting edge of galaxy evolution studies in the next decade and beyond.

References

[1] Koekemoer, A. M., Ellis, R. S., McLure, R. J., et al. 2013, The Astrophysical Journal Supplement, 209, 3

[2] Giavalisco, M., Ferguson, H. C., Koekemoer, A. M., et al. 2004, The Astrophysical Journal Letters, 600, L93

[3] Scoville, N., Aussel, H., Brusa, M., et al. 2007, The Astrophysical Journal Supplement, 172, 1

[4] Grogin, N. A., Kocevski, D. D., Faber, S. M., et al. 2011, The Astrophysical Journal Supplement, 197, 35

[5] Madau, P., & Dickinson, M. 2014, Annual Review of Astronomy and Astrophysics, 52, 415

[6] Mortlock, A., Conselice, C. J., Hartley, W. G., et al. 2013, Monthly Notices of the Royal Astronomical Society, 433, 1185

[7] Wisnioski, E., Förster Schreiber, N. M., Wuyts, S., et al. 2015, The Astrophysical Journal, 799, 209

[8] Behroozi, P. S., Wechsler, R. H., & Conroy, C. 2013, The Astrophysical Journal, 770, 57

[9] Wuyts, S., Förster Schreiber, N. M., Genzel, R., et al. 2012, The Astrophysical Journal, 753, 114

[10] Newman, S. F., Genzel, R., Förster Schreiber, N. M., et al. 2013, The Astrophysical Journal, 767, 104

[11] Jones, T. A., Swinbank, A. M., Ellis, R. S., Richard, J., & Stark, D. P. 2010, Monthly Notices of the Royal Astronomical Society, 404, 1247

[12] Bolton, A. S., Burles, S., Koopmans, L. V. E., Treu, T., & Moustakas, L. A. 2006, The Astrophysical Journal, 638, 703

[13] Coe, D., Benítez, N., Broadhurst, T., & Moustakas, L. A. 2010, The Astrophysical Journal, 723, 1678

[14] Zwicky, F. 1937, Physical Review, 51, 290

[15] Walsh, D., Carswell, R. F., & Weymann, R. J. 1979, Nature, 279, 381

[16] Schechter, P. L., Bailyn, C. D., Barr, R., et al. 1997, The Astrophysical Journal Letters, 475, L85

[17] Bayliss, M. B. 2012, The Astrophysical Journal, 744, 156

[18] Newman, A. B., Ellis, R. S., & Treu, T. 2015, The Astrophysical Journal, 814, 26

[19] Sonnenfeld, A., Treu, T., Gavazzi, R., et al. 2012, The Astrophysical Journal, 752, 163

[20] Lefor, A. T., Futamase, T., & Akhlaghi, M. 2013, New Astronomy Review, 57, 1

[21] Sand, D. J., Treu, T., Ellis, R. S., & Smith, G. P. 2005, The Astrophysical Journal, 627, 32

[22] Ebeling, H., Edge, A. C., & Henry, J. P. 2001, The Astrophysical Journal, 553, 668

[23] Gilbank, D. G., Gladders, M. D., Yee, H. K. C., & Hsieh, B. C. 2011, The Astronomical Journal, 141, 94

[24] Jauzac, M., Richard, J., Jullo, E., et al. 2015, Monthly Notices of the Royal Astronomical Society, 452, 1437

[25] Faure, C., Kneib, J.-P., Covone, G., et al. 2008, The Astrophysical Journal Supplement, 176, 19

[26] Belokurov, V., Evans, N. W., Hewett, P. C., et al. 2009, Monthly Notices of the Royal Astronomical Society, 392, 104

[27] Koester, B. P., Gladders, M. D., Hennawi, J. F., et al. 2010, The Astrophysical Journal Letters, 723, L73

[28] Kubo, J. M., Allam, S. S., Drabek, E., et al. 2010, The Astrophysical Journal Letters, 724, L137

[29] Stark, D. P., Auger, M., Belokurov, V., et al. 2013, Monthly Notices of the Royal Astronomical Society, 436, 1040

[30] Negrello, M., Hopwood, R., De Zotti, G., et al. 2010, Science, 330, 800

[31] Vieira, J. D., Marrone, D. P., Chapman, S. C., et al. 2013, Nature, 495, 344

[32] Wardlow, J. L., Cooray, A., De Bernardis, F., et al. 2013, The Astrophysical Journal, 762, 59

[33] Förster Schreiber, N. M., Genzel, R., Lehnert, M. D., et al. 2006, The Astrophysical Journal, 645, 1062

[34] Nesvadba, N. P. H., Lehnert, M. D., Eisenhauer, F., et al. 2006, The Astrophysical Journal, 650, 661

[35] Genzel, R., Tacconi, L. J., Eisenhauer, F., et al. 2006, Nature, 442, 786

[36] Genzel, R., Burkert, A., Bouché, N., et al. 2008, The Astrophysical Journal, 687, 59

[37] Förster Schreiber, N. M., Genzel, R., Bouché, N., et al. 2009, The Astrophysical Journal, 706, 1364

[38] Law, D. R., Steidel, C. C., Erb, D. K., et al. 2009, The Astrophysical Journal, 697, 2057

[39] Stark, D. P., Swinbank, A. M., Ellis, R. S., et al. 2008, Nature, 455, 775

[40] Jones, T., Ellis, R. S., Richard, J., & Jullo, E. 2013, The Astrophysical Journal, 765, 48

[41] Law, D. R., Steidel, C. C., Shapley, A. E., et al. 2012, The Astrophysical Journal, 745, 85

[42] Livermore, R. C., Jones, T. A., Richard, J., et al. 2015, Monthly Notices of the Royal Astronomical Society, 450, 1812

[43] Law, D. R., Shapley, A. E., Steidel, C. C., et al. 2012, Nature, 487, 338

[44] Yuan, T.-T., Kewley, L. J., Swinbank, A. M., Richard, J., & Livermore, R. C. 2011, The Astrophysical Journal Letters, 732, L14

[45] Förster Schreiber, N. M., Shapley, A. E., Genzel, R., et al. 2011, The Astrophysical Journal, 739, 45

[46] Wisnioski, E., Glazebrook, K., Blake, C., et al. 2012, Monthly Notices of the Royal Astronomical Society, 422, 3339

[47] Livermore, R. C., Jones, T., Richard, J., et al. 2012, Monthly Notices of the Royal Astronomical Society, 427, 688

[48] Dekel, A., Sari, R., & Ceverino, D. 2009, The Astrophysical Journal, 703, 785

[49] Genzel, R., Newman, S., Jones, T., et al. 2011, The Astrophysical Journal, 733, 101

[50] Newman, S. F., Shapiro Griffin, K., Genzel, R., et al. 2012, The Astrophysical Journal, 752, 111

[51] Dekel, A., Birnboim, Y., Engel, G., et al. 2009, Nature, 457, 451

[52] Goerdt, T., Ceverino, D., Dekel, A., & Teyssier, R. 2015, Monthly Notices of the Royal Astronomical Society, 454, 637

[53] Brooks, A. M., Governato, F., Quinn, T., Brook, C. B., & Wadsley, J. 2009, The Astrophysical Journal, 694, 396

[54] Danovich, M., Dekel, A., Hahn, O., Ceverino, D., & Primack, J. 2015, Monthly Notices of the Royal Astronomical Society, 449, 2087

[55] Genel, S., Naab, T., Genzel, R., et al. 2012, The Astrophysical Journal, 745, 11

[56] Dekel, A., & Krumholz, M. R. 2013, Monthly Notices of the Royal Astronomical Society, 432, 455

[57] Krumholz, M. R., & Dekel, A. 2010, Monthly Notices of the Royal Astronomical Society, 406, 112

[58] Erb, D. K., Steidel, C. C., Shapley, A. E., et al. 2006, The Astrophysical Journal, 646, 107

[59] Baker, A. J., Tacconi, L. J., Genzel, R., Lehnert, M. D., & Lutz, D. 2004, The Astrophysical Journal, 604, 125

[60] Daddi, E., Bournaud, F., Walter, F., et al. 2010, The Astrophysical Journal, 713, 686

[61] Tacconi, L. J., Neri, R., Genzel, R., et al. 2013, The Astrophysical Journal, 768, 74

[62] Saintonge, A., Lutz, D., Genzel, R., et al. 2013, The Astrophysical Journal, 778, 2

[63] Dessauges-Zavadsky, M., Zamojski, M., Schaerer, D., et al. 2015, Astronomy and Astrophysics, 577, A50

[64] Swinbank, A. M., Dye, S., Nightingale, J. W., et al. 2015, The Astrophysical Journal Letters, 806, L17

[65] Danielson, A. L. R., Swinbank, A. M., Smail, I., et al. 2013, Monthly Notices of the Royal Astronomical Society, 436, 2793

[66] Schaerer, D., Boone, F., Jones, T., et al. 2015, Astronomy and Astrophysics, 576, L2

[67] Jones, T., Stark, D. P., & Ellis, R. S. 2012, The Astrophysical Journal, 751, 51

[68] Jones, T. A., Ellis, R. S., Schenker, M. A., & Stark, D. P. 2013, The Astrophysical Journal, 779, 52

[69] Shapley, A. E. 2011, Annual Review of Astronomy and Astrophysics, 49, 525

[70] Pettini, M., Rix, S. A., Steidel, C. C., et al. 2002, The Astrophysical Journal, 569, 742

[71] Sales, L. V., Navarro, J. F., Schaye, J., et al. 2010, Monthly Notices of the Royal Astronomical Society, 409, 1541

[72] Erb, D. K. 2008, The Astrophysical Journal, 674, 151

[73] Henry, A., Scarlata, C., Domínguez, A., et al. 2013, The Astrophysical Journal Letters, 776, L27

[74] Davé, R., Finlator, K., & Oppenheimer, B. D. 2011, Monthly Notices of the Royal Astronomical Society, 416, 1354

[75] Jones, T., Wang, X., Schmidt, K. B., et al. 2015, The Astronomical Journal, 149, 107

[76] Vila-Costas, M. B., & Edmunds, M. G. 1992, Monthly Notices of the Royal Astronomical Society, 259, 121

[77] Gibson, B. K., Pilkington, K., Brook, C. B., Stinson, G. S., & Bailin, J. 2013, Astronomy and Astrophysics, 554, A47

[78] Anglés-Alcázar, D., Davé, R., Özel, F., & Oppenheimer, B. D. 2014, The Astrophysical Journal, 782, 84

[79] Leethochawalit, N., Jones, T. A., Ellis, R. S., et al. 2016, ApJ, 820, 84

[80] Yuan, T.-T., Kewley, L. J., & Rich, J. 2013, The Astrophysical Journal, 767, 106

[81] Stott, J. P., Sobral, D., Swinbank, A. M., et al. 2014, Monthly Notices of the Royal Astronomical Society, 443, 2695

[82] Finkelstein, S. L., Ryan, R. E., Jr., Papovich, C., et al. 2015, The Astrophysical Journal, 810, 71

[83] McLeod, D. J., McLure, R. J., Dunlop, J. S., et al. 2015, Monthly Notices of the Royal Astronomical Society, 450, 3032

[84] Robertson, B. E., Ellis, R. S., Furlanetto, S. R., & Dunlop, J. S. 2015, The Astrophysical Journal Letters, 802, L19

[85] Postman, M., Coe, D., Benítez, N., et al. 2012, The Astrophysical Journal Supplement, 199, 25

[86] Bradač, M., Ryan, R., Casertano, S., et al. 2014, The Astrophysical Journal, 785, 108

[87] Treu, T., Schmidt, K. B., Brammer, G. B., et al. 2015, The Astrophysical Journal, 812, 114

[88] Bayliss, M. B., Sharon, K., & Johnson, T. 2015, The Astrophysical Journal Letters, 802, L9

[89] Ebeling, H. 2015, IAU General Assembly, 22, #2256512

[90] Marshall, P. J., Verma, A., More, A., et al. 2016, Monthly Notices of the Royal Astronomical Society, 455, 1171